Cell Mol Neurobiol
DOI 10.1007/s10571-016-0437-1

ORIGINAL RESEARCH

Olfactory Ensheathing Cell-Conditioned Medium Reverts $A\beta_{25-35}$-Induced Oxidative Damage in SH-SY5Y Cells by Modulating the Mitochondria-Mediated Apoptotic Pathway

Qing-Qing Fu[1] · Li Wei[2] · Javier Sierra[3] · Jian-Zhang Cheng[1] · María Teresa Moreno-Flores[4] · Hua You[5] · Hua-Rong Yu[1]

Received: 31 August 2016 / Accepted: 18 October 2016

Abstract Olfactory ensheathing cells (OECs) are a type of glia from the mammalian olfactory system, with neuroprotective and regenerative properties. β-Amyloid peptides are a major component of the senile plaques characteristic of the Alzheimer brain. The amyloid beta (Aβ) precursor protein is cleaved to amyloid peptides, and $A\beta_{25-35}$ is regarded to be the functional domain of Aβ, responsible for its neurotoxic properties. It has been reported that $A\beta_{25-35}$ triggers reactive oxygen species (ROS)-mediated oxidative damage, altering the structure and function of mitochondria, leading to the activation of the mitochondrial intrinsic apoptotic pathway. Our goal is to investigate the effects of OECs on the toxicity of aggregated $A\beta_{25-35}$, in human neuroblastoma SH-SY5Y cells. For such purpose, SH-SY5Y cells were incubated with $A\beta_{25-35}$ and OEC-conditioned medium (OECCM). OECCM promoted the cell viability and reduced the apoptosis, and decreased the intracellular ROS and the lipid peroxidation. In the presence of OECCM, mRNA and protein levels of antioxidant enzymes (SOD1 and SOD2) were upregulated. Concomitantly, OECCM decreased mRNA and the protein expression levels of cytochrome c, caspase-9, caspase-3, and Bax in SH-SY5Y cells, and increased mRNA and the protein expression level of Bcl-2. However, OECCM did not alter intracellular Ca^{2+} concentration in SH-SY5Y cells. Taken together, our data suggest that OECCM ameliorates $A\beta_{25-35}$-induced oxidative damage in neuroblastoma SH-SY5Y cells by inhibiting the mitochondrial intrinsic pathway. These data provide new insights into the functional actions of OECCM on oxidative stress-induced cell damage.

Keywords Alzheimer's disease · Olfactory ensheathing cells · $A\beta_{25-35}$ · Oxidative damage · Mitochondria · Apoptosis

Qing-Qing Fu and Li Wei have contributed equally to this work.

Electronic supplementary material The online version of this article (doi:10.1007/s10571-016-0437-1) contains supplementary material, which is available to authorized users.

✉ Hua You
youhua307@163.com

✉ Hua-Rong Yu
huarongyu2003@163.com

Qing-Qing Fu
1129142449@qq.com

Li Wei
weilikw@163.com

Javier Sierra
j.sierra.prof@ufv.es

Jian-Zhang Cheng
1037367895@qq.com

María Teresa Moreno-Flores
mteresa.moreno@uam.es

[1] Research Center of Neuroscience, Chongqing Medical University, Chongqing 400016, China

[2] Key Laboratory of Birth Defects and Reproductive Health of the National Health and Family Planning Commission, Chongqing Population and Family Planning Science and Technology Research Institute, Chongqing 400020, China

[3] Faculty of Experimental Sciences, Universidad Francisco de Vitoria, Pozuelo de Alarcón, 28223 Madrid, Spain

[4] Department of Anatomy, Histology and Neuroscience, Faculty of Medicine, Universidad Autónoma de Madrid, 28029 Madrid, Spain

[5] Affiliated Hospital of the Academy of Military Medical Sciences, Beijing 100071, China

Journal : Large 10571 | Dispatch : 28-10-2016 | Pages : 12
Article No. : 437 | LE | TYPESET
MS Code : CEMN-D-16-00309 | CP | DISK

Introduction

Alzheimer's disease (AD) is a progressive neurodegenerative disorder, clinically characterized by cognitive decline, which includes impairment in learning, episodic memory, decision making and orientation (Blennow et al. 2006). One of the major histopathological features of AD is the accumulation of extracellular amyloid plaques that are composed principally of fibrillar β-amyloid (Aβ) peptide. Aβ is a small protein, a byproduct of amyloid precursor protein (APP) processing, with $A\beta_{40}$ being the more frequent isoform seen in aggregates. Specifically, $A\beta_{25–35}$ is the key toxic fragment of the full-length Aβ peptide (Jamasbi et al. 2016; Yang et al. 2016). Aβ peptide aggregation toxicity is due, among others, to oxidative injury, apoptosis, mitochondrial dysfunction, disruption of signaling pathways, and Ca^{2+} homeostasis disturbance, eventually leading to neuronal death and cognitive impairment (Sun et al. 2015). Increased levels of Aβ can be used as an early diagnostic indicator of early preclinical stage of AD (Scheff et al. 2016).

There is an ample body of literature supporting a crucial role for mitochondrial dysfunction in AD, with altered energy metabolism and reactive oxygen species (ROS) production being the major correlates (Moreira et al. 2010; Lin and Beal 2006). It is widely believed that Aβ is responsible for these mitochondrial alterations, although the mechanism has not yet been fully elucidated (Moreira et al. 2010). It is generally accepted that Aβ could elevate oxidative stress and induce apoptotic cell death by initiating mitochondrial dysfunction, which is associated with the changes in the proteins of Bcl-2 family, release of cytochrome c, and activation of caspase-3 (Butterfield et al. 2013).

Superoxide dismutase enzymes (SOD1 and SOD2) are the major lines of antioxidant defense against Aβ-induced ROS toxicity (Yang et al. 2016). They, along with other antioxidants such as metal chelators or glutathione peroxidases, have been shown to be essential for neuronal survival and protection against oxidative damage and can be used to treat cognitive and behavioral symptoms of AD (Gonzalez-Zulueta et al. 1998). In addition, antioxidants have been hypothesized to protect against $A\beta_{25–35}$-induced toxicity in AD (Jung Choi et al. 2009; Fan et al. 2016).

Licensed treatments and examples of emerging treatments for AD were summarized as symptomatic (cholinesterase inhibitors, NMDA receptor antagonist), neuropsychiatric (atypical antipsychotics, antidepressants, anticonvulsants) and disease-modifying treatments (immunotherapy, secretase inhibitors, amyloid inhibitors, copper or zinc modulators, tau aggregation inhibitors, GSK3 inhibitors, natural products, and vitamins) (Ballard et al. 2011). However, there is no effective treatment to cure this disease hitherto. At present, cell transplantation strategy is considered as the most promising treatment strategy for AD (Sugaya et al. 2006; Oliveira and Hodges 2005). Mesenchymal stromal cells (Lee et al. 2009, 2012; Eftekharzadeh et al. 2015; Wu et al. 2007), neural progenitor cells (Zhang et al. 2015; Lee et al. 2015), and embryonic stem cells (Yue et al. 2015) have been used in the animal model of AD, and shown to obtain beneficial effects.

OECs are capable of ensheathing and guiding newly growing axons of olfactory sensory neurons, from the olfactory mucosa to their targets in the CNS during mammalian lifespan (Moreno-Flores et al. 2003b; Woodhall et al. 2001; Doucette et al. 1983; Nedelec et al. 2005). For this reason, many attempts to repair damage in the injured CNS have relied on OEC grafts (Barnett and Chang 2004; Moreno-Flores et al. 2002; Ekberg and St John 2014). Previous studies suggested that OEC could induce axonal regeneration after CNS injury and promote functional recovery in the injured spinal cord (Moreno-Flores and Avila 2006; Moreno-Flores et al. 2006; Garcia-Escudero et al. 2011; Li et al. 1997; Ramon-Cueto et al. 1998, 2000). The precise mechanisms accounting for the observed recovery are not fully understood but may include neuroprotection, reduction of the glial scar, promotion of axonal regeneration, and remyelination (Roet and Verhaagen 2014; Reginensi et al. 2015). Previously, Moreno-Flores et al. and other groups established immortalized OEC clonal cell lines, TEG3, conserving the pro-regenerative capacity of primary OEC with promising potential for their therapeutic use (Moreno-Flores and Avila 2006; Pastrana et al. 2007, 2006; Garcia-Escudero et al. 2011; Moreno-Flores et al. 2003a, b).

OECs produce growth factors, nerve growth factor (NGF), brain-derived neurotrophic factor (BDNF), glial cell-derived neurotrophic factor (GDNF), and ciliary neurotrophic factor (CNTF), cell adhesion molecules, and extracellular matrix proteins that are beneficial for axonal regeneration (Woodhall et al. 2001; Pellitteri et al. 2009; Pastrana et al. 2006). Olfactory ensheathing cell-conditioned medium (OECCM) reverts SH-SY5Y damage induced by 6 hydroxydopamine (6OHDA) (Shukla et al. 2014) and astrocyte damage induced by H_2O_2 (Jinbo et al. 2013; Liu et al. 2013). Furthermore, OECCM increased oligodendroglial and neuronal differentiation of neural progenitor cells (Carvalho et al. 2014) and human mesenchymal stem cells (Zeng et al. 2013), respectively.

In the present study, we show that OECCM from TEG3 counteracts against $A\beta_{25–35}$-induced oxidative damage in SH-SY5Y cells. Analysis of mitochondrial apoptosis-related genes allows us to propose that such effect is rendered via the modulation of the intrinsic apoptotic pathway.

Journal : Large 10571 | Dispatch : 28-10-2016 | Pages : 12
Article No. : 437 | LE | TYPESET
MS Code : CEMN-D-16-00309 | CP | DISK

Materials and Methods

SH-SY5Y Cells Culture

SH-SY5Y cells were maintained in a humidified incubator at 37 °C with 5 % CO_2 in Dulbecco's Modified Eagle's Medium (DMEM) (Hyclone, Logan, UT, USA) supplemented with 10 % Fetal bovine serum (FBS) (Tian Jin Hao Yang Biological Manufacture CO., Tianjin, China) and 1 % penicillin–streptomycin (Beyotime Biotechnology, Nantong, China).

TEG3 Culture

Moreno-Flores et al. have previously described the isolation of the immortalized clonal cell line, TEG3, which is a SV40 large T antigen-stable transfectant of OEC primary cultures prepared from adult rat olfactory bulbs (Moreno-Flores et al. 2003a, b). TEG3 cells were maintained in DMEM supplemented with 10 % FBS and 1 % penicillin–streptomycin.

OECCM and Heat-Inactivated OECCM Preparation

TEG3 cells were maintained in DMEM containing 10 % FBS onto uncoated 25 cm^2 culture flasks (Corning, New York, USA) at 37 °C in 5 % CO_2. When the cell culture reached about 80 % confluence, the conditioned medium was collected, filtered through a membrane of 0.2 mm pore (Jinbo et al. 2013), aliquoted and stored at −20 °C. The same method was used to generate the conditioned medium from HeLa cells and HEK293 cells as controls, called HeLaCM and HEKCM, respectively. OECCM was boiled for 10 min at 100 °C to generate heat-inactivated OECCM (HOECCM).

Preparation of Aged $A\beta_{25–35}$ and Cell Treatment

As previously described by us (Yang et al. 2016), $A\beta_{25–35}$ (Sangon Biotech, Shanghai, China) was dissolved in sterilized, double-distilled, water at a concentration of 1 mM and incubated in a capped vial at 37 °C for 7 days to form an aggregated form. As reported in our previous study (Yang et al. 2016), exposure of SH-SY5Y cells to $A\beta_{25–35}$ (40 μM) for 6 h resulted in approximately 50 % cell death. SH-SY5Y cells were treated with aged 40 μM $A\beta_{25–35}$ and OECCM for 6 h, simultaneously. The complete culture medium was mixed with OECCM according to the ratio of 1:1 before usage. Cells cultured without any treatment were used as controls.

CCK8 Assay

Cell viability was measured by CCK8 assay (cell counting kit-8, Dojindo Molecular Technologies, Tokyo, Japan). The SH-SY5Y cells were seeded at 1×10^4 cells per well in 100 μl of complete growth culture media. Cells were then exposed to 40 μM $A\beta_{25–35}$ or 40 μM $A\beta_{25–35}$ + OECCM for 6 h. Finally, CCK-8 solution (10 μl/well) was added to the wells. After 2-h incubation at 37 °C, the absorbance of each well was determined at 450 nm using a microplate reader.

Detection of Apoptosis with Flow Cytometry

Apoptosis assay kit was purchased from KeyGen Biotechnology (Nanjing, China). SH-SY5Y cells were treated as described above, then collected after digestion with 0.25 % trypsin without EDTA, and washed twice with PBS (phosphate buffer saline). To the pellets of SH-SY5Y cells were successively added 500 μl Binding Buffer, 5 μl Annexin V-FITC, and 5 μl Propidium iodide (PI), and then incubated for 10 min at room temperature in a dark environment. The signals of FITC and PI were detected by FL1 (FITC detector) and FL2 (phycoerythrin fluorescence detector) at 488 and 561 nm, respectively, mounted on a a Beckman Gallios flow cytometer (Beckman Coulter, California, USA).

Intracellular Reactive Oxygen Species (ROS) Level

SH-SY5Y cells were treated as described above. ROS were detected using the cell-permeable, peroxide-sensitive fluorophore (Life Technologies, USA), according to the manufacturer's instructions. SH-SY5Y cells were incubated with 5 μmol/l CellROX Orange reagent for 30 min at 37 °C and then washed twice with pre-warmed PBS. A Beckman Gallios flow cytometer (Beckman Coulter, California, USA) was used to measure ROS by the fluorescence emission of the CellROX dye. The cultured cells were illuminated at 488 nm and emitted at 525–530 nm. The reported fluorescence intensity values were expressed as the arithmetic mean of the results ± standard deviation (SD), and were determined for 10,000 analyzed cells.

Analysis of Lipid Peroxidation

SH-SY5Y cells were treated as described above, after which we analyzed cell lipid peroxidation. Polyunsaturated lipids are susceptible to an oxidative attack, typically by ROS, resulting in a chain reaction with the production of end products such as malondialdehyde (MDA). We determined lipid peroxidation by quantifying the amount of cellular MDA via the measurement of a red-complex produced during the reaction of thiobarbituric acid (TBA) with MDA.

Journal : Large 10571 Dispatch : 28-10-2016 Pages : 12
Article No. : 437 LE TYPESET
MS Code : CEMN-D-16-00309 CP DISK

A microplate reader (UV-7504, Shanghai, China) was used to measure the absorbance of cellular MDA at 532 nm, and the MDA content was calculated according to the detailed instructions of the MDA assay kit (Nanjing Jiancheng Bioengineering Institute, Nanjing, China).

Enzyme Activity Assays

SH-SY5Y cells were treated as described above for the ROS level tests, after which we assayed the enzyme activity. The activities of three enzymes: superoxide dismutase (SOD; EC1.15.1.1), glutathione peroxidase (GPx; EC 1.11.1.9), and catalase (CAT; EC1.11.1.6) were determined using commercial kits according to the manufacturer's protocols (Nanjing Jiancheng Bioengineering Institute, Nanjing, China). Enzyme activity assays were carried out using a UV–Visible spectrophotometer (UV-7504, Shanghai, China).

Calcium Imaging

SH-SY5Y cells were treated as described above, and we then used calcium imaging to determine intracellular free Ca^{2+} concentration ($[Ca^{2+}]_i$) using Fluo-4 AM (Dojindo Molecular Technologies, Tokyo, Japan). In brief, the prepared cells were loaded with the fluorescent calcium probe Fluo-4 AM (5 μM) in the dark for 30 min at 37 °C, washed twice with PBS, and finally centrifuged at 1000 rpm for 3 min to remove free Fluo-4 AM. Fluo-4 AM-loaded cells were resuspended and incubated for 20 min at 37 °C. They were then illuminated at 488 nm, and the emission light at 530 nm was detected.

Quantitative Real-Time Fluorescence Polymerase Chain Reaction (q-PCR)

SH-SY5Y cells were treated and collected as described above. Total RNA was extracted from SH-SY5Y cells with Trizol reagent (TaKaRa, Tokyo, Japan). First-strand complementary DNA (cDNA) was synthesized using the Reverse transcription Kit (TaKaRa, Tokyo, Japan) according to manufacturer's instructions. For quantitative PCR (q-PCR), 10 μl reaction system including 5 μl 2 × SYBR Green (TaKaRa, Tokyo, Japan), 0.8 μl cDNA templates, and 0.8 μl q-PCR primers set were used. The samples were run and analyzed in triplicate using CFX Connect Real-Time System (Bio-Rad, Hercules, USA). The q-PCR conditions were as follows: an initial 3-min denaturation step at 95 °C, followed by the sequence of 40 cycles of 95 °C for 5 s, 58 °C for 30 s, and 72 °C for 30 s. The primer sets used are listed in Supplementary Table 1. Melting curve analysis showed a single amplification peak for each reaction. C_t values for targets were expressed as relative expressions compared to the averages of housekeeping genes (GAPDH). The expression of each mRNA was calculated as $2^{-\Delta\Delta C_t}$.

Western Blot

Total protein was prepared from the cultures in RIPA Lysis Buffer (CWBio, Beijing, China). After maintaining the samples for 20 min on ice, BCA protein assay (Beyotime Biotech, Jiangsu, China) was used to determine the protein concentration. Equal amounts of proteins from SH-SY5Y cells of each sample were resolved by SDS-PAGE on 12 % polyacrylamide gels and then electrotransfered to PVDF membranes (Millipore Corp, USA). After blocking the membranes in 5 % non-fat dry milk in Tris-buffered saline with 0.1 % Tween 20 (TBST) for 2 h, the membranes were incubated with the following primary antibodies at 4 °C overnight: anti-SOD1 (1:1000, Immunoway, USA), anti-SOD2 (1:500, Wanleibio, Liaoning, China), anti-cytochrome c (1:500, Wanleibio, Liaoning, China), anti-caspase-9 (1:500, Wanleibio, Liaoning, China), anti-caspase-3 (1:500, Wanleibio, Liaoning, China), anti-Bax (1:1000, Wanleibio, Liaoning, China), anti-Bcl-2 (1:1000, Wanleibio, Liaoning, China), and β-actin (1:500, Immunoway, USA). Then, the membranes were washed with TBST five times and incubated with a secondary antibody which was conjugated to horseradish peroxidase for 2 h at room temperature. Protein bands were detected using an enhanced chemiluminescence kit (Beyotime Biotech, Jiangsu, China) and imaged using a Molecular Imager ChemiDoc XRS system (Bio-Rad). Signals were quantified using densitometric analyses with Quantity One analysis software (BioRad), and results are expressed as optical density arbitrary units.

Immunofluorescence

SH-SY5Y cells were cultured on cover-slips, fixed with 4 % paraformaldehyde at room temperature for 20 min, washed three times with PBS, and finally permeabilized with PBS containing 2 % Triton-X100 for 10 min. Cells were incubated with the following primary antibodies at 4 °C overnight: Bax (1:150, Immunoway, USA) and Bcl-2 (1:150, Wanleibio, Liaoning, China). After washing with PBS, SH-SY5Y cells were further incubated with the secondary antibody conjugated to anti-rabbit Dylight 488 (1:1000, Abbkine, California, USA) for 2 h. Cell nuclei were stained with DAPI for 10 min. Finally, the cover-slips were washed and mounted with fluoromount. The cells were visualized using an inverted fluorescent microscope (Leica, Germany). Median Fluorescence Intensity was analyzed using Image J software, and results expressed as the arithmetic means of the optical densities (arbitrary units) ± standard deviation (SD), and were determined for ten preparations.

Journal : Large 10571 | Dispatch : 28-10-2016 | Pages : 12
Article No. : 437 | ☐ LE | ☐ TYPESET
MS Code : CEMN-D-16-00309 | ☑ CP | ☑ DISK

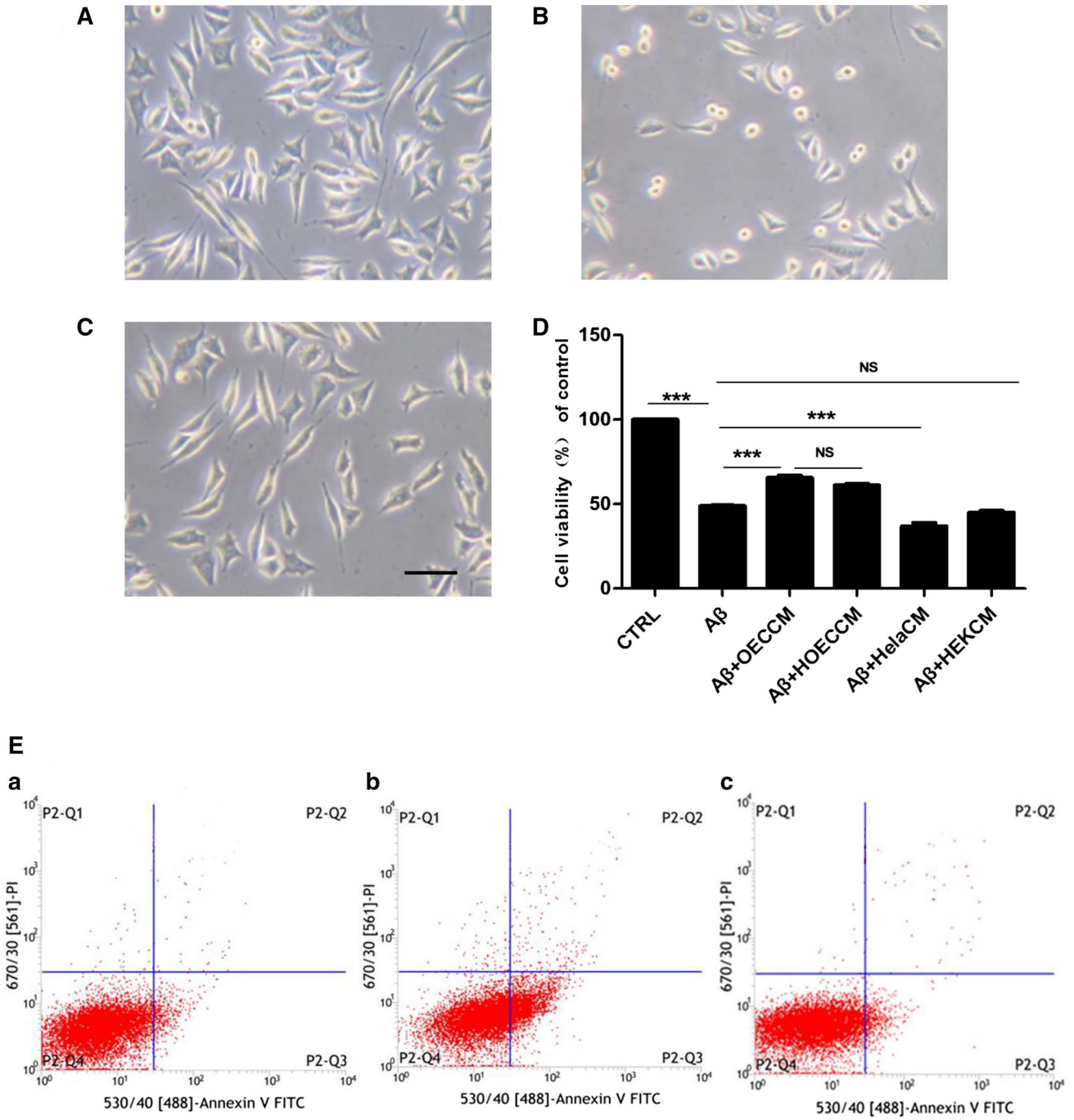

Fig. 1 OECCM reduces $A\beta_{25-35}$-induced cell death in SH-SY5Y cells by decreasing apoptosis. Cell viability was analyzed by CCK8 in control cells (**A**), $A\beta_{25-35}$-alone-treated SH-SY5Y cells (**B**), and $A\beta_{25-35}$ + OECCM-treated SH-SY5Y cells (**C**). The results were compared among control cells (CTRL), $A\beta_{25-35}$-alone-treated SH-SY5Y cells (Aβ), $A\beta_{25-35}$ + OECCM-treated SH-SY5Y cells (Aβ + OECCM), $A\beta_{25-35}$ + heat-inactivated OECCM-treated SH-SY5Y cells (Aβ + HOECCM), $A\beta_{25-35}$ + HeLaCM-treated SH-SY5Y cells (Aβ + HeLaCM), and $A\beta_{25-35}$ + HEKCM-treated SH-SY5Y cells (Aβ + HEKCM) (**D**). Data are expressed as the mean ± SD ($n = 6$). $*p < 0.05$, $***p < 0.001$, no significance is indicated as "NS". *Scale bar* 20 μm. Cell apoptosis was detected by flow cytometry in control cells (**Ea**), $A\beta_{25-35}$ alone-treated SH-SY5Y cells (**Eb**) and in $A\beta_{25-35}$ + OECCM-treated SH-SY5Y cells (**Ec**)

Statistical Analysis

All experiments were conducted at least in triplicate, and representative data are expressed as the mean ± SD. The comparisons were evaluated by one-way analysis of variance, and for those significant, post-hoc multiple comparisons between means was realized with Turkey test. All statistical analyses were performed using SPSS statistics

Journal : Large 10571 | Dispatch : 28-10-2016 | Pages : 12
Article No. : 437 | LE | TYPESET
MS Code : CEMN-D-16-00309 | CP | DISK

22.0 software, and values of $p < 0.05$ were considered to be significant. All graphs were drawn by using the software Graphpad Prism 5.3.

Results

OECCM Reduces $A\beta_{25-35}$-Induced Cell Death in SH-SY5Y Cells by Decreasing Apoptosis

$A\beta_{25-35}$-alone-treated cells displayed shrinkage, round cell body, and smaller body size than normal cells. OECCM + $A\beta_{25-35}$-treated cells showed similar morphology to normal cells (Fig. 1A–C). While cell viability for $A\beta_{25-35}$-treated cells was lower than control cells (CTRL), OECCM reduced significantly $A\beta_{25-35}$-induced cell death compared with $A\beta_{25-35}$-alone-treated cells (Fig. 1D). Surprisingly, HOECCM also showed similar protective effects with OECCM (Fig. 1D). No beneficial potential was observed with HeLaCM and HEKCM (Fig. 1D).

Next we looked at cellular apoptosis in different conditions, by flow cytometry. In the scatter of the flow cytometry results, the lower left quadrant represents normal cells (AnnexinV-FITC-/PI−), the lower right quadrant represents early apoptotic cells (AnnexinV-FITC+/PI−), and the upper right quadrant represents the late apoptotic and necrotic cells (AnnexinV-FITC+/PI+)(Jinbo et al. 2013). Compared with control (Fig. 1Ea), exposure of SH-SY5Y cells to $A\beta_{25-35}$ resulted in an increase of cell death with approximately 29.9 % of cells in apoptosis (7.1 % in the early and 22.8 % in the late apoptotic stage) (Fig. 1Eb). Concomitant OECCM treatment reduced $A\beta_{25-35}$-induced death resulting in 8.6 % cell apoptosis (3.9 % of early and 5.4 % of late apoptotic cell) (Fig. 1Ec).

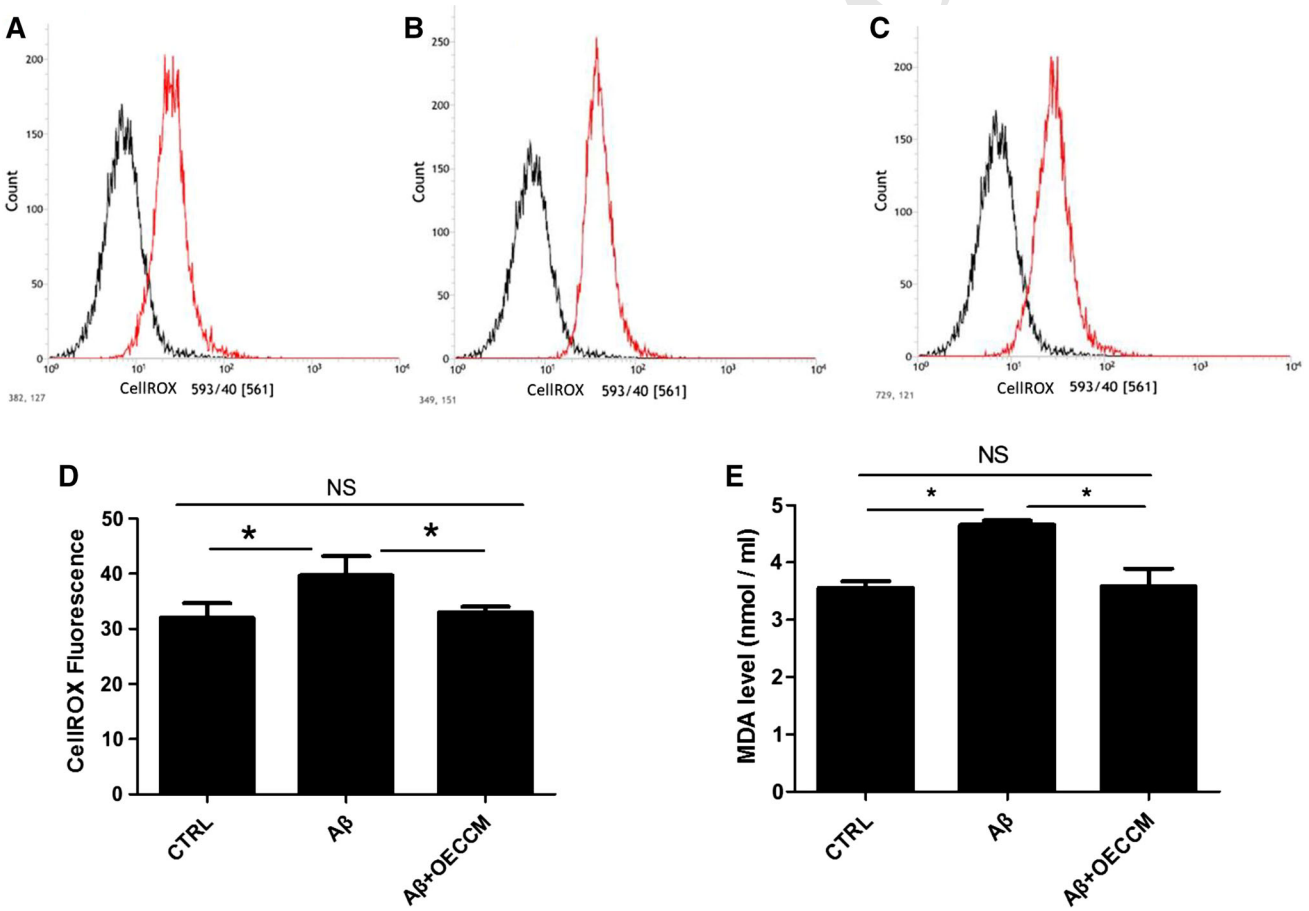

Fig. 2 OECCM decreases ROS generation in SH-SY5Y cells. The generation of reactive oxygen species was analyzed by flow cytometry in normal cells (**A**), $A\beta_{25-35}$-alone-treated SH-SY5Y cells (**B**) and $A\beta_{25-35}$ + OECCM-treated SH-SY5Y cells (**C**), and the results were compared across the different treatments (**D**). Data are expressed as the mean ± SD of CellROX Fluorescence intensity ($n = 3$). **E** The levels of malondialdehyde (MDA) in the cell supernatant were measured by a UV–Visible spectrophotometer ($n = 5$). *$p < 0.05$, no significance is indicated as "NS"

Journal : Large 10571 Dispatch : 28-10-2016 Pages : 12
Article No. : 437 LE TYPESET
MS Code : CEMN-D-16-00309 CP DISK

OECCM Decreases ROS Generation in SH-SY5Y Cells

The accumulation of ROS has been observed in $A\beta_{25-35}$-induced cell toxicity, and mitochondria have been considered to be sensitive targets for ROS (Yang et al. 2016). To determine whether OECCM could decrease the intracellular ROS levels, we used a ROS-sensitive dye, CellROX Orange. Exposure to $A\beta_{25-35}$ resulted in significantly higher ROS levels in SH-SY5Y cells (Fig. 2B) compared with controls (Fig. 2A, D). ROS levels were significantly lower in $A\beta_{25-35}$ + OECCM-treated SH-SY5Y cells (Fig. 2C, D) than those in cells treated with $A\beta_{25-35}$ alone (Fig. 2B). There was no significant difference of ROS levels between normal cells and the OECCM-treated cells (Fig. 2D).

Because oxidative stress has been shown to trigger and sustain the pathogenesis of $A\beta_{25-35}$-induced cell toxicity, we examined whether OECCM treatment decreased oxidative stress induced by $A\beta_{25-35}$. For such purpose, we analyzed lipid peroxidation by determining the MDA level. There is a significant increase of MDA levels in SH-SY5Y cells treated with $A\beta_{25-35}$, relative to non-treated cells. These levels return to control conditions in $A\beta_{25-35}$ + OECCM-treated SH-SY5Y cells (Fig. 2E).

OECCM Modulates the Redox State in SH-SY5Y

We also investigated whether treatment could restore antioxidant status, by determining the enzymatic activities and gene expression of SOD, CAT, and GPx. We further detected the protein levels of two important anti-oxidative enzymes, SOD1 and SOD2.

Exposure to $A\beta_{25-35}$ resulted in significantly lower levels of total SOD, CAT, and GPx enzymatic activities, compared with non-treated cells. These activities significantly increase in $A\beta_{25-35}$ + OECCM-treated SH-SY5Y cells (Fig. 3A). After treatment with $A\beta_{25-35}$, the gene expression levels ($2^{-\Delta\Delta C_t}$) of SOD1, SOD2, CAT, and GPx suffer a significant reduction. Such expression levels are partially restored by OECCM, with a significant increase in $A\beta_{25-35}$ + OECCM-treated SH-SY5Y cells relative to $A\beta_{25-35}$-treated cells (Fig. 3B). The same conclusion was reached when protein levels of SOD1 and SOD2 were determined (Fig. 3C, D) by Western Blot.

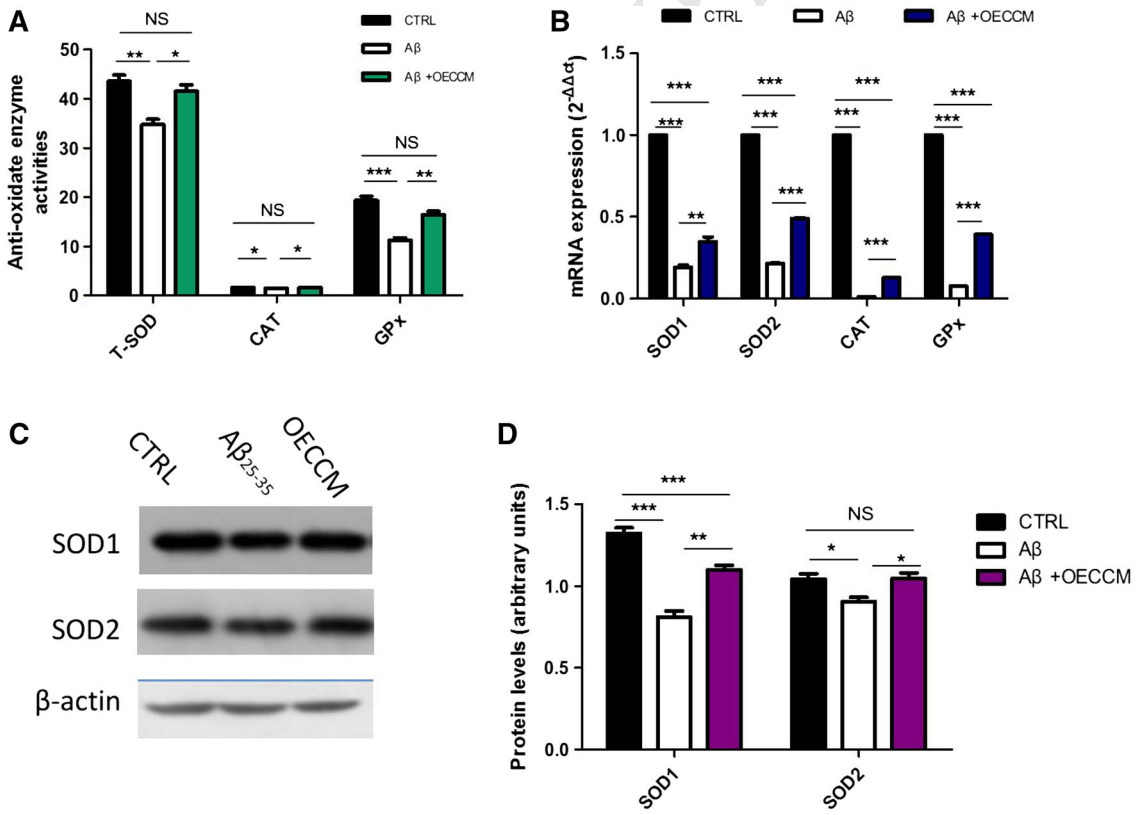

Fig. 3 OECCM modulates the redox state of SH-SY5Y cells exposed to $A\beta_{25-35}$. **A** Enzymatic activities of total SOD (T-SOD), CAT, and GP_x. **B** mRNA levels of endogenous antioxidant enzyme genes were detected by q-PCR. The expression of each mRNA was calculated as $2^{-\Delta\Delta C_t}$, and the mRNA levels of SOD1 and SOD2, CAT, and GPx were normalized with the mRNA levels of GAPDH. **C**, **D** SOD1 and SOD2 protein levels were detected by Western blot, and were normalized with the expression level of β-actin. Data are expressed as mean of arbitrary units ± SD ($n = 3$). $*p < 0.05$, $**p < 0.01$, $***p < 0.001$, no significance is indicated as "NS"

Journal : Large 10571 Dispatch : 28-10-2016 Pages : 12
Article No. : 437 LE TYPESET
MS Code : CEMN-D-16-00309 CP DISK

OECCM Does Not Alter Ca^{2+} Concentration in SH-SY5Y cells

Ca^{2+} overload is associated with mitochondrial dysfunction, which contributes to apoptosis. There was no significant difference in intracellular Ca^{2+} concentration among control cells, $A\beta_{25-35}$ -alone-treated cells and $A\beta_{25-35}$ + OECCM-treated cells, as demonstrated by flow cytometry (Fig. 4A, B).

OECCM Prevents the $A\beta_{25-35}$-Induced Activation of the Mitochondria-Mediated Apoptosis Pathway in SH-SY5Y Cells

Mitochondria-mediated apoptosis has been suggested to be involved in $A\beta_{25-35}$-induced cell toxicity. We therefore investigated whether the beneficial role of OECCM in preventing $A\beta_{25-35}$-induced SH-SY5Y cell death involved the inhibition of the mitochondria-mediated apoptosis pathway. Mitochondria-mediated apoptosis requires the interplay of a number of pro- and anti-apoptotic B cell lymphoma-2 (Bcl-2) family proteins and the caspase cascade (Soriano and Scorrano 2011). To assess the status of the mitochondria-mediated apoptosis pathway, we measured the levels of pro-apoptotic molecules cytochrome c, caspase-3, caspase-9, and Bax, as well as the anti-apoptotic molecule Bcl-2 in SH-SY5Y cells, by q-PCR and Western blotting.

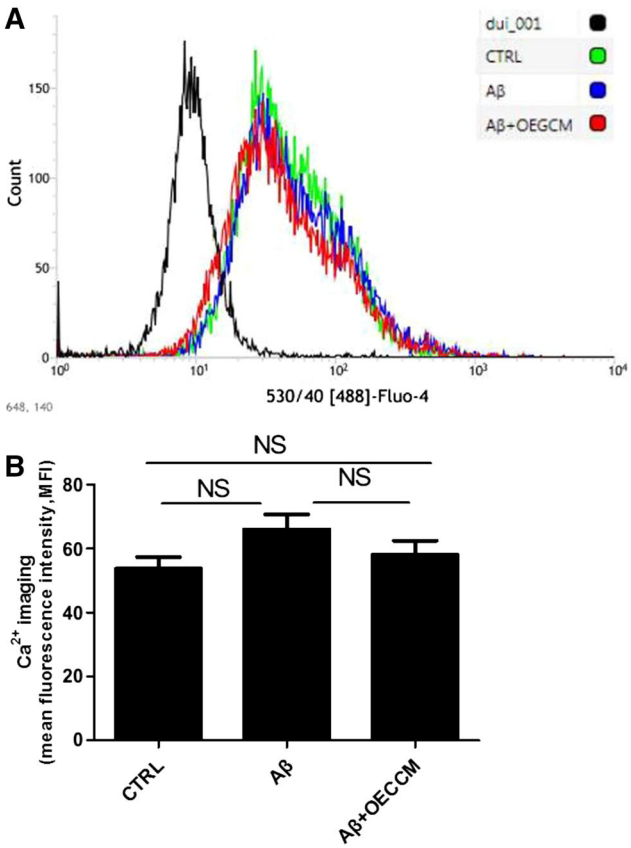

Fig. 4 OECCM does not alter Ca^{2+} concentration in SH-SY5Y cells. [Ca^{2+}] was analyzed using Ca^{2+} imaging in control cells, $A\beta_{25-35}$-alone-treated SH-SY5Y cells, and $A\beta_{25-35}$ + OECCM-treated SH-SY5Y cells (**A**). The results were compared between different treatments (**B**). Data are expressed as the mean ± SD ($n = 3$). No significance is indicated as "NS"

Exposure of cells to $A\beta_{25-35}$ resulted in significantly higher mRNA levels of cytochrome c, caspase-9, caspase-3, and Bax with respect to control cells (Fig. 5A), as well as a protein increase for the same conditions (Fig. 5B, C). As expected, lower expression levels of the anti-apoptotic Bcl-2 gene (mRNA and protein) were observed in SH-SY5Y + $A\beta_{25-35}$ cells compared with controls (Fig. 5A, B). On the contrary, SH-SY5Y cells treated with $A\beta_{25-3}$ + OECCM had significantly lower gene expression levels (mRNA and protein) of cytochrome c, caspase-9, caspase-3, and Bax than those from cells treated with $A\beta_{25-35}$ alone (Fig. 5A–C). Opposite results were obtained for Bcl-2, for which mRNA and protein levels were significantly higher in $A\beta_{25-35}$ + OECCM-treated cells than those in cells treated with $A\beta_{25-35}$ alone (Fig. 5A–C).

We also performed immune fluorescence staining of pro-apoptotic molecule Bax and anti-apoptotic molecule Bcl-2 (Fig. 6A) and quantified mean fluorescence intensity (MFI) using Image J software (Fig. 6B, C). Exposure of the cells to $A\beta_{25-35}$ resulted in significantly higher MFI level of Bax and lower MIF level of Bcl-2 in $A\beta_{25-35}$-treated SH-SY5Y cells compared with controls. The MIF levels of Bax and Bcl-2 in $A\beta_{25-35}$ + OECCM-treated SH-SY5Y cells were significantly lower and higher, respectively, than those in the cells treated with $A\beta_{25-35}$ alone (Fig. 6A–C).

In summary, our data demonstrate that OECCM treatment resulted in a 42.55 % improvement in all parameters tested compared to those in cells treated with $A\beta_{25-35}$ alone, OECCM treatment resulted in 77.41 % restoration in all parameters tested compared to those in control untreated cells, and $A\beta_{25-35}$ resulted in a 64.77 % deterioration in all parameters tested compared to those in control cells (Supplementary Table 2).

Discussion

AD, a neurodegenerative disease associated with aging, is considered to be the most common form of dementia. The cause of AD involves the accumulation of Aβ, oxidative stress, inflammation, and dysfunction in several processes including hormonal and mitochondrial pathways (Doraiswamy 2002). The increased proteolytic degradation of APP and aggregation and deposition of Aβ are considered to be two characteristic pathologies in the development and

Journal : Large 10571 | Dispatch : 28-10-2016 | Pages : 12
Article No. : 437 | LE | TYPESET
MS Code : CEMN-D-16-00309 | CP | DISK

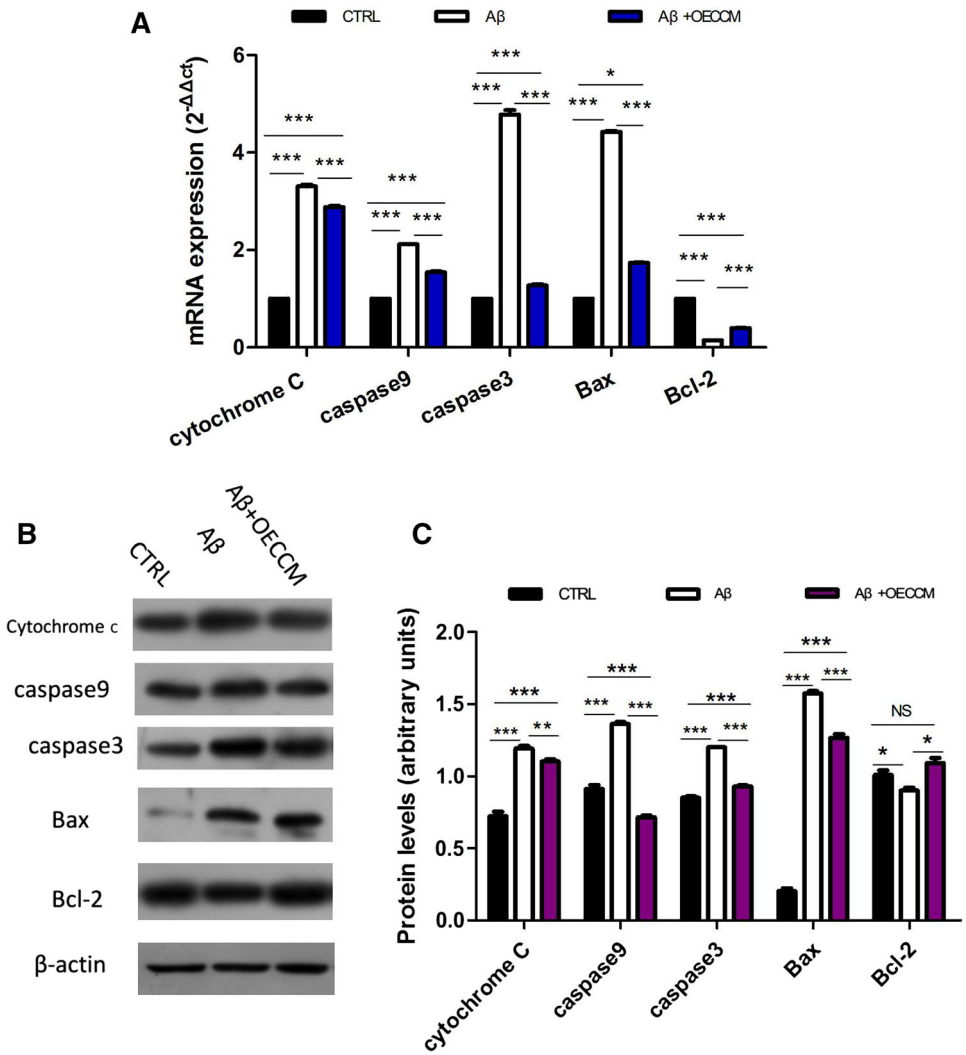

Fig. 5 OECCM prevents the $A\beta_{25-35}$-induced activation of the mitochondria-mediated apoptosis pathway in SH-SY5Y cells. **A** mRNA levels of mitochondrial apoptotic-related molecules were examined by q-PCR—cytochrome c, caspase-9, caspase-3, Bax, and Bcl-2—and were normalized to the expression level of GAPDH. Data are expressed as the mean ± SD (n = 3). $*p < 0.05$, $***p < 0.001$; no significance is indicated as "NS". **B**, **C** Protein levels of cytochrome c, caspase-9, caspase-3, Bax, and Bcl-2 were examined by western blot and were normalized to the expression level of β-actin. Data are expressed as the mean ± SD ($n = 3$). $*p < 0.05$, $**p < 0.01$, $***p < 0.001$; no significance is indicated as "NS"

progression of AD (Tsunekawa et al. 2008). Aβ plays a role in synaptic dysfunction and neuronal death and therefore contributes to cognitive impairment (Roher et al. 2009).

Specifically, $A\beta_{25-35}$ is the core toxic fragment of the full-length Aβ peptide (Yang et al. 2016) and can permeate through the cell membrane relatively more easily due to its smaller size. In addition, its toxicity is similar to those of $A\beta_{1-40}$ and $A\beta_{1-42}$ (Mattson et al. 1997). More importantly, $A\beta_{25-35}$ is a particularly intractable peptide because it aggregates rapidly, unlike the full-length Aβ, which requires aging for more than 1 week before it aggregates and becomes toxic (Hughes et al. 2000). As such, it is often used for in vitro studies of the neuroprotective effects of various drugs predicted to modulate Aβ toxicity (Yu et al. 2014).

It is reported that OECCM is able to promote the survival and the neurite outgrowth of hippocampal neurons in vitro (Pellitteri et al. 2009), and it has the capacity to protect SH-SY5Y damage induced by 6OHDA (Shukla et al. 2014) and astrocyte damage induced by H_2O_2 (Jinbo et al. 2013; Liu et al. 2013). Furthermore, OECCM further increased the differentiation function of neural progenitor cells (Carvalho et al. 2014) and human mesenchymal stem cells (Zeng et al. 2013) into oligodendrocytes and neurons, respectively. As OEC-conditioned media are a source of growth factors, we believed that these positive beneficial biological effects of OECCM may be mediated by some protein/s in a paracrine manner (Woodhall et al. 2001). Surprisingly, in the present study, we found that heat-inactivated OECCM presented a similar level of protective potential compared with OECCM. Thus, the beneficial effects of OECCM for SH-SY5Y cells exposed to $A\beta_{25-35}$ may be brought out through peptide/s or heat-resistant protein/s (Kim et al. 2000). Alternatively, it may be the effect of molecules protected from heat inactivation inside lipidic vesicles, for example, exosomes (Nafar et al. 2015; Martín-Duque P. personal communication). Further studies are needed to address this issue.

Journal : Large 10571 | Dispatch : 28-10-2016 | Pages : 12
Article No. : 437 | LE | TYPESET
MS Code : CEMN-D-16-00309 | CP | DISK

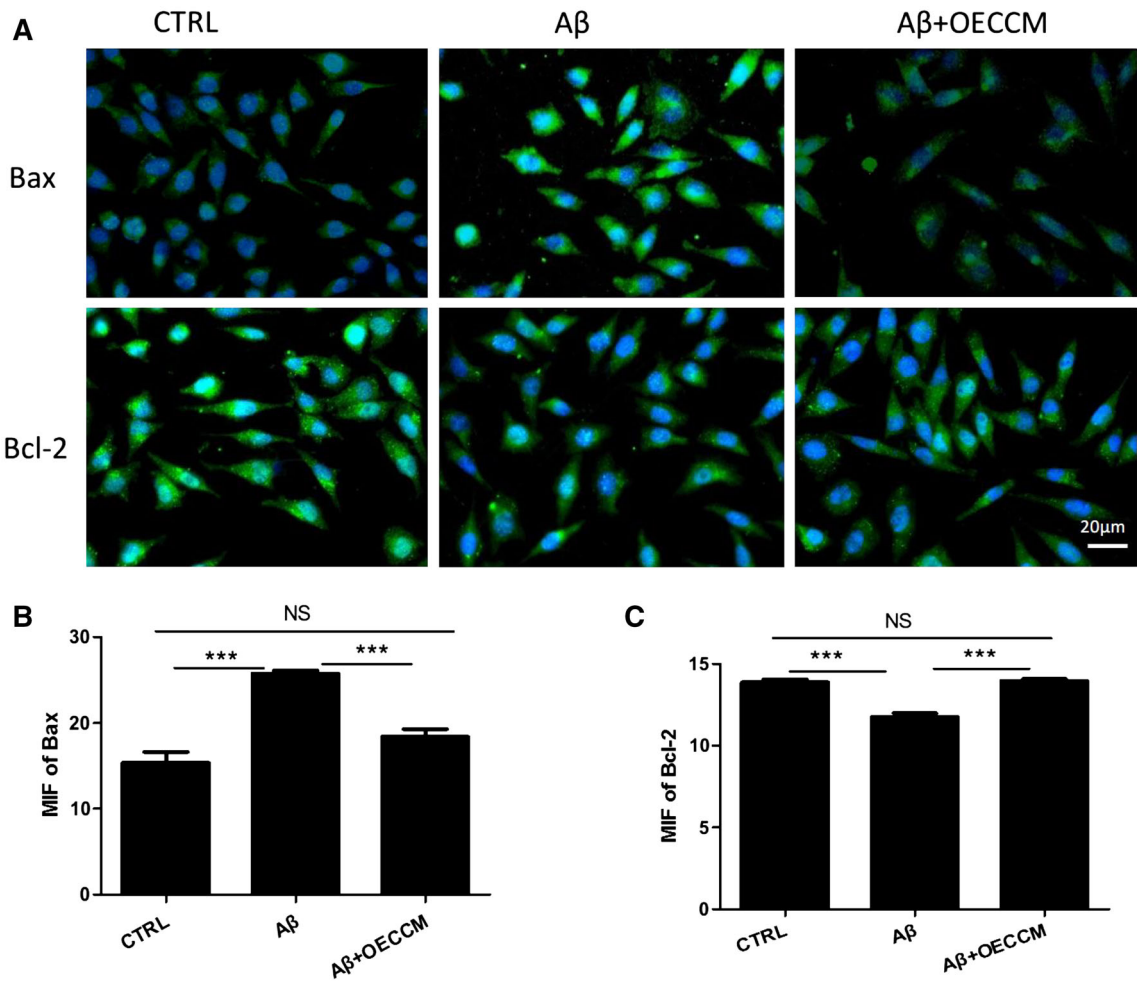

Fig. 6 OECCM reverts the $A\beta_{25-35}$-induced activation of the pro-apoptotic molecule Bax and inhibition of anti-apoptotic molecule Bcl-2 in SH-SY5Y cells. The pro-apoptotic molecule Bax and anti-apoptotic molecule Bcl-2 were also examined by immunofluorescence staining (**A**), and their median fluorescence intensity (MFI) was analyzed by Image J software (**B** and **C**). Data are expressed as the mean ± SD ($n = 10$). ***$p < 0.001$, no significance is indicated as "NS". *Scale bar* 20 μm

The generation of ROS leading to oxidative damage and neuronal cell death plays an important role in the pathogenesis of neurodegenerative disorders, and antioxidants have been proposed to protect against $A\beta_{25-35}$-induced toxicity in AD (Jung Choi et al. 2009). Lipid peroxidation and antioxidant activities of SOD enzymes in brain tissue from patients with AD and age-matched controls, were determined in different brain regions: SOD activity was significantly decreased in frontal and temporal cortex of AD (Marcus et al. 1998). In the present study, ROS production increased after $A\beta_{25-35}$ exposure and decreased after OECCM treatment. $A\beta_{25-35}$ exposure resulted in reduction of mRNA levels of SOD1, SOD2, GPx, and CAT; protein levels of SOD1 and SOD2; and activities of total SOD, CAT, and GPx in SH-SY5Y cells. Interestingly, OECCM restored normal levels of antioxidant enzymes system. This observation indicates a positive feedback loop in the antioxidant enzymes system of SH-SY5Y cells, being activated by OECCM in response to $A\beta_{25-35}$.

Mitochondrial dysfunction has been correlated to AD, its main factors being altered energy metabolism and ROS production (Moreira et al. 2010; Lin and Beal 2006). Aβ could elevate oxidative stress and induce apoptotic cell death by initiating mitochondrial dysfunction, which is associated with changes in proteins of Bcl-2 family, release of cytochrome c, and activation of caspase-3 (Butterfield et al. 2013). In the present study, we used q-PCR and Western blot to measure the RNA and protein levels of mitochondria-mediated apoptosis markers. We found that $A\beta_{25-35}$ increased the expressions at mRNA and protein levels of cytochrome c, caspase-3, caspase-9, and Bax, and decreased mRNA and protein levels of protective Bcl-2. $A\beta_{25-35}$ + OECCM-treated cells partially recovered expression levels of mitochondria-mediated apoptosis

Journal : Large 10571 Dispatch : 28-10-2016 Pages : 12
Article No. : 437 LE TYPESET
MS Code : CEMN-D-16-00309 CP DISK

markers, indicating that OECCM prevented $A\beta_{25-35}$-induced SH-SY5Y cell death through inhibition of mitochondrial apoptosis pathway.

In summary, we have demonstrated that OECCM ameliorated $A\beta_{25-35}$-induced oxidative damage in neuroblastoma SH-SY5Y cells through inhibition of the mitochondria-dependent pathway and provided new insights into the paracrine actions of OECs in oxidative stress-induced cell damage. To the best of our knowledge, this is the first study to evaluate and highlight the protective action of OEC against $A\beta_{25-35}$-induced cell insult.

Funding This work was supported by grants from the National Natural Science Foundation of China (81670180, 81370077 and 81001220), the cutting-edge research project of the Chongqing Science and Technology Committee (CSTC2014JCYJA10014), the Scientific and Technological Research Programme of Chongqing Municipal Education Commission (KJ130320), NIG Collaborative Research Program (2016-A2-4), the Chongqing Science and Technology Committee (CSTC2016JCYJA0083), Beijing Municipal Science and Technology Commission, and Chongqing Municipal Commission of Health and Family Planning (2016MSXM103). The funders had no role in the study design, data collection and analysis, decision to publish, or preparation of the manuscript.

References

Ballard C, Gauthier S, Corbett A, Brayne C, Aarsland D, Jones E (2011) Alzheimer's disease. Lancet 377(9770):1019–1031. doi:10.1016/s0140-6736(10)61349-9

Barnett SC, Chang L (2004) Olfactory ensheathing cells and CNS repair: going solo or in need of a friend? Trends Neurosci 27(1):54–60. doi:10.1016/j.tins.2003.10.011

Blennow K, de Leon MJ, Zetterberg H (2006) Alzheimer's disease. Lancet 368(9533):387–403. doi:10.1016/s0140-6736(06)69113-7

Butterfield DA, Swomley AM, Sultana R (2013) Amyloid beta-peptide (1-42)-induced oxidative stress in Alzheimer disease: importance in disease pathogenesis and progression. Antioxid Redox Signal 19(8):823–835. doi:10.1089/ars.2012.5027

Carvalho LA, Vitorino LC, Guimaraes RP, Allodi S, de Melo Reis RA, Cavalcante LA (2014) Selective stimulatory action of olfactory ensheathing glia-conditioned medium on oligodendroglial differentiation, with additional reference to signaling mechanisms. Biochem Biophys Res Commun 449(3):338–343. doi:10.1016/j.bbrc.2014.05.051

Doraiswamy PM (2002) Non-cholinergic strategies for treating and preventing Alzheimer's disease. CNS Drugs 16(12):811–824

Doucette JR, Kiernan JA, Flumerfelt BA (1983) The re-innervation of olfactory glomeruli following transection of primary olfactory axons in the central or peripheral nervous system. J Anat 137(Pt 1):1–19

Eftekharzadeh M, Nobakht M, Alizadeh A, Soleimani M, Hajghasem M, Kordestani Shargh B, Karkuki Osguei N, Behnam B, Samadikuchaksaraei A (2015) The effect of intrathecal delivery of bone marrow stromal cells on hippocampal neurons in rat model of Alzheimer's disease. Iran J Basic Med Sci 18(5):520–525

Ekberg JA, St John JA (2014) Crucial roles for olfactory ensheathing cells and olfactory mucosal cells in the repair of damaged neural tracts. Anat Rec 297(1):121–128. doi:10.1002/ar.22803

Fan CD, Li Y, Fu XT, Wu QJ, Hou YJ, Yang MF, Sun JY, Fu XY, Zheng ZC, Sun BL (2016) Reversal of beta-amyloid-induced neurotoxicity in PC12 cells by curcumin, the important role of ROS-mediated signaling and ERK pathway. Cell Mol Neurobiol. doi:10.1007/s10571-016-0362-3

Garcia-Escudero V, Gargini R, Gallego-Hernandez MT, Garcia-Gomez A, Martin-Bermejo MJ, Simon D, Delicado A, Moreno-Flores MT, Avila J, Lim F (2011) A neuroregenerative human ensheathing glia cell line with conditional rapid growth. Cell Transplant 20(2):153–166. doi:10.3727/096368910x522108

Gonzalez-Zulueta M, Ensz LM, Mukhina G, Lebovitz RM, Zwacka RM, Engelhardt JF, Oberley LW, Dawson VL, Dawson TM (1998) Manganese superoxide dismutase protects nNOS neurons from NMDA and nitric oxide-mediated neurotoxicity. J Neurosci 18(6):2040–2055

Hughes E, Burke RM, Doig AJ (2000) Inhibition of toxicity in the beta-amyloid peptide fragment beta-(25-35) using N-methylated derivatives: a general strategy to prevent amyloid formation. J Biol Chem 275(33):25109–25115. doi:10.1074/jbc.M003554200

Jamasbi E, Wade JD, Separovic F, Hossain MA (2016) Amyloid beta (Abeta) peptide and factors that play important roles in Alzheimer's disease. Curr Med Chem 23(9):884–892

Jinbo L, Zhiyuan L, Zhijian Z, WenGe D (2013) Olfactory ensheathing cell-conditioned medium protects astrocytes exposed to hydrogen peroxide stress. Cell Mol Neurobiol 33(5):699–705. doi:10.1007/s10571-013-9937-4

Jung Choi S, Kim MJ, Jin Heo H, Kim JK, Jin Jun W, Kim HK, Kim EK, Ok Kim M, Yon Cho H, Hwang HJ, Jun Kim Y, Shin DH (2009) Ameliorative effect of 1,2-benzenedicarboxylic acid dinonyl ester against amyloid beta peptide-induced neurotoxicity. Amyloid 16(1):15–24. doi:10.1080/13506120802676997

Kim TD, Ryu HJ, Cho HI, Yang CH, Kim J (2000) Thermal behavior of proteins: heat-resistant proteins and their heat-induced secondary structural changes. Biochemistry 39(48):14839–14846

Lee JK, Jin HK, Bae JS (2009) Bone marrow-derived mesenchymal stem cells reduce brain amyloid-beta deposition and accelerate the activation of microglia in an acutely induced Alzheimer's disease mouse model. Neurosci Lett 450(2):136–141. doi:10.1016/j.neulet.2008.11.059

Lee HJ, Lee JK, Lee H, Carter JE, Chang JW, Oh W, Yang YS, Suh JG, Lee BH, Jin HK, Bae JS (2012) Human umbilical cord blood-derived mesenchymal stem cells improve neuropathology and cognitive impairment in an Alzheimer's disease mouse model through modulation of neuroinflammation. Neurobiol Aging 33(3):588–602. doi:10.1016/j.neurobiolaging.2010.03.024

Lee IS, Jung K, Kim IS, Lee H, Kim M, Yun S, Hwang K, Shin JE, Park KI (2015) Human neural stem cells alleviate Alzheimer-like pathology in a mouse model. Mol Neurodegener 10:38. doi:10.1186/s13024-015-0035-6

Li Y, Field PM, Raisman G (1997) Repair of adult rat corticospinal tract by transplants of olfactory ensheathing cells. Science 277(5334):2000–2002

Lin MT, Beal MF (2006) Mitochondrial dysfunction and oxidative stress in neurodegenerative diseases. Nature 443(7113):787–795. doi:10.1038/nature05292

Liu J, Qiu J, Xiong Y, Liu Z, Gao J (2013) The mitochondrial protective mechanism of olfactory ensheathing cells conditioned medium protects against H_2O_2-induced injury in astrocytes. Neurosci Lett 555:91–96. doi:10.1016/j.neulet.2013.09.011

Marcus DL, Thomas C, Rodriguez C, Simberkoff K, Tsai JS, Strafaci JA, Freedman ML (1998) Increased peroxidation and reduced antioxidant enzyme activity in Alzheimer's disease. Exp Neurol 150(1):40–44. doi:10.1006/exnr.1997.6750

Journal : Large 10571 | Dispatch : 28-10-2016 | Pages : 12
Article No. : 437 | LE | TYPESET
MS Code : CEMN-D-16-00309 | CP | DISK

Mattson MP, Begley JG, Mark RJ, Furukawa K (1997) Abeta25-35 induces rapid lysis of red blood cells: contrast with Abeta1-42 and examination of underlying mechanisms. Brain Res 771(1):147–153

Moreira PI, Carvalho C, Zhu X, Smith MA, Perry G (2010) Mitochondrial dysfunction is a trigger of Alzheimer's disease pathophysiology. Biochim Biophys Acta 1802(1):2–10. doi:10.1016/j.bbadis.2009.10.006

Moreno-Flores MT, Avila J (2006) The quest to repair the damaged spinal cord. Recent Pat CNS Drug Discov 1(1):55–63

Moreno-Flores MT, Diaz-Nido J, Wandosell F, Avila J (2002) Olfactory ensheathing glia: drivers of axonal regeneration in the central nervous system? J Biomed Biotechnol 2(1):37–43. doi:10.1155/s1110724302000372

Moreno-Flores MT, Lim F, Martin-Bermejo MJ, Diaz-Nido J, Avila J, Wandosell F (2003a) High level of amyloid precursor protein expression in neurite-promoting olfactory ensheathing glia (OEG) and OEG-derived cell lines. J Neurosci Res 71(6):871–881. doi:10.1002/jnr.10527

Moreno-Flores MT, Lim F, Martin-Bermejo MJ, Diaz-Nido J, Avila J, Wandosell F (2003b) Immortalized olfactory ensheathing glia promote axonal regeneration of rat retinal ganglion neurons. J Neurochem 85(4):861–871

Moreno-Flores MT, Bradbury EJ, Martin-Bermejo MJ, Agudo M, Lim F, Pastrana E, Avila J, Diaz-Nido J, McMahon SB, Wandosell F (2006) A clonal cell line from immortalized olfactory ensheathing glia promotes functional recovery in the injured spinal cord. Mol Ther 13(3):598–608. doi:10.1016/j.ymthe.2005.11.014

Nafar F, Williams JB, Mearow KM (2015) Astrocytes release HspB1 in response to amyloid-β exposure in vitro. J Alzheimers Dis 49(1):251–263. doi:10.3233/JAD-150317

Nedelec S, Dubacq C, Trembleau A (2005) Morphological and molecular features of the mammalian olfactory sensory neuron axons: what makes these axons so special? J Neurocytol 34(1–2):49–64. doi:10.1007/s11068-005-5047-7

Oliveira AA Jr, Hodges HM (2005) Alzheimer's disease and neural transplantation as prospective cell therapy. Curr Alzheimer Res 2(1):79–95

Pastrana E, Moreno-Flores MT, Gurzov EN, Avila J, Wandosell F, Diaz-Nido J (2006) Genes associated with adult axon regeneration promoted by olfactory ensheathing cells: a new role for matrix metalloproteinase 2. J Neurosci 26(20):5347–5359. doi:10.1523/jneurosci.1111-06.2006

Pastrana E, Moreno-Flores MT, Avila J, Wandosell F, Minichiello L, Diaz-Nido J (2007) BDNF production by olfactory ensheathing cells contributes to axonal regeneration of cultured adult CNS neurons. Neurochem Int 50(3):491–498. doi:10.1016/j.neuint.2006.10.004

Pellitteri R, Spatuzza M, Russo A, Zaccheo D, Stanzani S (2009) Olfactory ensheathing cells represent an optimal substrate for hippocampal neurons: an in vitro study. Int J Dev Neurosci 27(5):453–458. doi:10.1016/j.ijdevneu.2009.05.001

Ramon-Cueto A, Plant GW, Avila J, Bunge MB (1998) Long-distance axonal regeneration in the transected adult rat spinal cord is promoted by olfactory ensheathing glia transplants. J Neurosci 18(10):3803–3815

Ramon-Cueto A, Cordero MI, Santos-Benito FF, Avila J (2000) Functional recovery of paraplegic rats and motor axon regeneration in their spinal cords by olfactory ensheathing glia. Neuron 25(2):425–435

Reginensi D, Carulla P, Nocentini S, Seira O, Serra-Picamal X, Torres-Espin A, Matamoros-Angles A, Gavin R, Moreno-Flores MT, Wandosell F, Samitier J, Trepat X, Navarro X, del Rio JA (2015) Increased migration of olfactory ensheathing cells secreting the Nogo receptor ectodomain over inhibitory substrates and lesioned spinal cord. Cell Mol Life Sci 72(14):2719–2737. doi:10.1007/s00018-015-1869-3

Roet KC, Verhaagen J (2014) Understanding the neural repair-promoting properties of olfactory ensheathing cells. Exp Neurol 261:594–609. doi:10.1016/j.expneurol.2014.05.007

Roher AE, Esh CL, Kokjohn TA, Castano EM, Van Vickle GD, Kalback WM, Patton RL, Luehrs DC, Daugs ID, Kuo YM, Emmerling MR, Soares H, Quinn JF, Kaye J, Connor DJ, Silverberg NB, Adler CH, Seward JD, Beach TG, Sabbagh MN (2009) Amyloid beta peptides in human plasma and tissues and their significance for Alzheimer's disease. Alzheimer's Dement 5(1):18–29. doi:10.1016/j.jalz.2008.10.004

Scheff SW, Ansari MA, Mufson EJ (2016) Oxidative stress and hippocampal synaptic protein levels in elderly cognitively intact individuals with Alzheimer's disease pathology. Neurobiol Aging 42:1–12. doi:10.1016/j.neurobiolaging.2016.02.030

Shukla A, Mohapatra TM, Parmar D, Seth K (2014) Neuroprotective potentials of neurotrophin rich olfactory ensheathing cell's conditioned media against 6OHDA-induced oxidative damage. Free Radic Res 48(5):560–571. doi:10.3109/10715762.2014.894636

Soriano ME, Scorrano L (2011) Traveling bax and forth from mitochondria to control apoptosis. Cell 145(1):15–17. doi:10.1016/j.cell.2011.03.025

Sugaya K, Alvarez A, Marutle A, Kwak YD, Choumkina E (2006) Stem cell strategies for Alzheimer's disease therapy. Panminerva Med 48(2):87–96

Sun X, Chen WD, Wang YD (2015) Beta-Amyloid: the key peptide in the pathogenesis of Alzheimer's disease. Front Pharmacol 6:221. doi:10.3389/fphar.2015.00221

Tsunekawa H, Noda Y, Mouri A, Yoneda F, Nabeshima T (2008) Synergistic effects of selegiline and donepezil on cognitive impairment induced by amyloid beta (25-35). Behav Brain Res 190(2):224–232. doi:10.1016/j.bbr.2008.03.002

Woodhall E, West AK, Chuah MI (2001) Cultured olfactory ensheathing cells express nerve growth factor, brain-derived neurotrophic factor, glia cell line-derived neurotrophic factor and their receptors. Mol Brain Res 88(1–2):203–213

Wu QY, Li J, Feng ZT, Wang TH (2007) Bone marrow stromal cells of transgenic mice can improve the cognitive ability of an Alzheimer's disease rat model. Neurosci Lett 417(3):281–285. doi:10.1016/j.neulet.2007.02.092

Yang R, Wei L, Fu QQ, You H, Yu HR (2016) SOD3 ameliorates Abeta25-35-induced oxidative damage in SH-SY5Y cells by Inhibiting the mitochondrial pathway. Cell Mol Neurobiol. doi:10.1007/s10571-016-0390-z

Yu H, Yao L, Zhou H, Qu S, Zeng X, Zhou D, Zhou Y, Li X, Liu Z (2014) Neuroprotection against Abeta25-35-induced apoptosis by *Salvia miltiorrhiza* extract in SH-SY5Y cells. Neurochem Int 75:89–95. doi:10.1016/j.neuint.2014.06.001

Yue W, Li Y, Zhang T, Jiang M, Qian Y, Zhang M, Sheng N, Feng S, Tang K, Yu X, Shu Y, Yue C, Jing N (2015) ESC-derived basal forebrain cholinergic neurons ameliorate the cognitive symptoms associated with Alzheimer's disease in mouse models. Stem Cell Rep 5(5):776–790. doi:10.1016/j.stemcr.2015.09.010

Zeng Y, Rong M, Liu Y, Liu J, Lu M, Tao X, Li Z, Chen X, Yang K, Li C, Liu Z (2013) Electrophysiological characterisation of human umbilical cord blood-derived mesenchymal stem cells induced by olfactory ensheathing cell-conditioned medium. Neurochem Res 38(12):2483–2489. doi:10.1007/s11064-013-1186-x

Zhang Q, Wu HH, Wang Y, Gu GJ, Zhang W, Xia R (2015) Neural stem cell transplantation decreases neuroinflammation in a transgenic mouse model of Alzheimer's disease. J Neurochem. doi:10.1111/jnc.13413

Journal : Large 10571 | Dispatch : 28-10-2016 | Pages : 12
Article No. : 437 | ☐ LE | ☐ TYPESET
MS Code : CEMN-D-16-00309 | ☑ CP | ☑ DISK